Magnetic characterization of layered $Ba_6Mn_5O_{16}$ and $Ba_4Mn_3O_{10}$

K. Boulahya, M. Parras, and J. M. González-Calbet*
Departamento de Química Inorgánica, Facultad de Químicas, Universidad Complutense, E-28040-Madrid, Spain

U. Amador
Departamento de Química, Facultad de Ciencias Experimentales y de la Salud, Universidad San Pablo-CEU, E-28668 Madrid, Spain

J. L. Martínez
Instituto de Ciencia de Materiales de Madrid, CSIC, Cantoblanco, E-28049 Madrid, Spain

M. T. Fernández-Díaz
Institut Laue Langevin, BP 156X, F-38042 Grenoble, France

(Received 29 July 2003; revised manuscript received 6 October 2003; published 30 January 2004)

Polycrystalline $Ba_6Mn_5O_{16}$ has been characterized by neutron diffraction and magnetic measurements. The structural essential feature of $Ba_6Mn_5O_{16}$ is the presence of zigzag layers perpendicular to [010] separated by Ba atoms and folded along the *c* axis. The layers are built up from (Mn_5O_{18}) units constituted by five face-sharing octahedra connected via their apices by two of their three terminal corners at each end of the (Mn_5O_{18}) group. The $Ba_6Mn_5O_{16}$ magnetic structure, determined from the neutron diffraction data, suggests a strong antiferromagnetic coupling within the (Mn_5O_{18}) units, and also an antiferromagnetic coupling between the different layers along [010]. $Ba_6Mn_5O_{16}$ presents a long-range three-dimensional antiferromagnetic order below $T_N = 87$ K. Around this temperature, the specific heat is comparable to that shown by $Ba_4Mn_3O_{10}$, the difference being related to the different number of the magnetic atoms in each case. From the magnetic specific heat, the value of the entropy associated with the antiferromagnetic ordering is obtained for both layered phases.

DOI: 10.1103/PhysRevB.69.024418 PACS number(s): 75.50.Ee, 61.12.Ld

INTRODUCTION

One of the last momentous events related to the perovskite structural type has been the discovery of colossal magnetoresistance (CMR) in manganese related perovskites. Following the observation of CMR in the three-dimensional $La_{1-x}Ca_xMnO_3$ system,[1] research into the magnetic transport properties of manganese mixed oxides was extended to layered Ruddlesden-Popper manganites.[2] Different structures can be stabilized in the *A*-Mn-O (*A* = alkaline-earth) system as a function of the chemical nature of the *A* ion, the *A*/Mn ratio and the oxygen content. For *A* = Ba, many perovskite-like oxides have been reported. $BaMnO_3$,[3] isotypic with $CsNiF_3$,[4] crystallizes in the one-dimensional 2H structural type. The introduction of anionic vacancies in this structure gives rise to an increase of the structural dimensionality.[5–8] The variation of the Ba/Mn ratio also affects the dimensionality of the structures. In this sense, two new layered manganates ($Ba_4Mn_3O_{10}$ and $Ba_6Mn_5O_{16}$) have been recently reported, opening new research routes in the fruitful Ba-Mn-O system.

$Ba_4Mn_3O_{10}$,[9] isotypic to $Cs_4Ni_3F_{10}$,[10] is built up from $[Mn_3O_{12}]$ units of three sharing-faces octahedra. Two of these units are linked via their apices through two of their three terminal corners [Fig. 1(a)]. The magnetic properties of this material are the outcome of intratrimer and intertrimer interactions. At high temperatures, the magnetic susceptibility of $Ba_4Mn_3O_{10}$ obeys the Curie-Weiss law; at 130 K, a broad maximum is observed in the susceptibility, probably caused by short-range spin pairing within the layers. Finally, long-range magnetic ordering seems to occur at 40 K. Neutron diffraction results confirm this ordered situation at 5 K where the antiferromagnetic (AFM) structure has been solved.[9]

$Ba_6Mn_5O_{16}$,[11] which constitutes the only example of a layered oxide isotypic to $Cs_6Ni_5F_{16}$,[12] is made from the same building principles of $Ba_4Mn_3O_{10}$ but the layers are now formed by (Mn_5O_{18}) units of five octahedra sharing faces. These units are linked via their apices, in a similar way than in $Ba_4Mn_3O_{10}$, as shown in Fig. 1(b).

In this paper, the magnetic structure of $Ba_6Mn_5O_{16}$, solved from neutron diffraction data, and its magnetic behavior are described. In addition, a comparative study of this phase with $Ba_4Mn_3O_{10}$ is reported.

EXPERIMENTAL DETAILS

High resolution neutron diffraction data were obtained on the D20 powder diffractometer at the Institute Laue Langevin (Grenoble, France), which is equipped with a multidetector (1600 counters) and works at a wavelength of 2.40 Å. The angular range covered by the detector expands from 2° to 154° in scattering angle (step size 0.10°). The temperature was changed sequentially from 2 to 300 K.

$Ba_6Mn_5O_{16}$ and $Ba_4Mn_3O_{10}$ were synthesized as polycrystalline samples by heating stoichiometric amounts of $BaCO_3$ (Aldrich 99.98%) and MnO_2 (Aldrich 99+%) in air at 1250 and 1350 °C, respectively, for three days and then quenched to room temperature. The chemical composition was analyzed by inductive coupling plasma and an energy-dispersive x-ray analysis. In both cases, the metal composi-

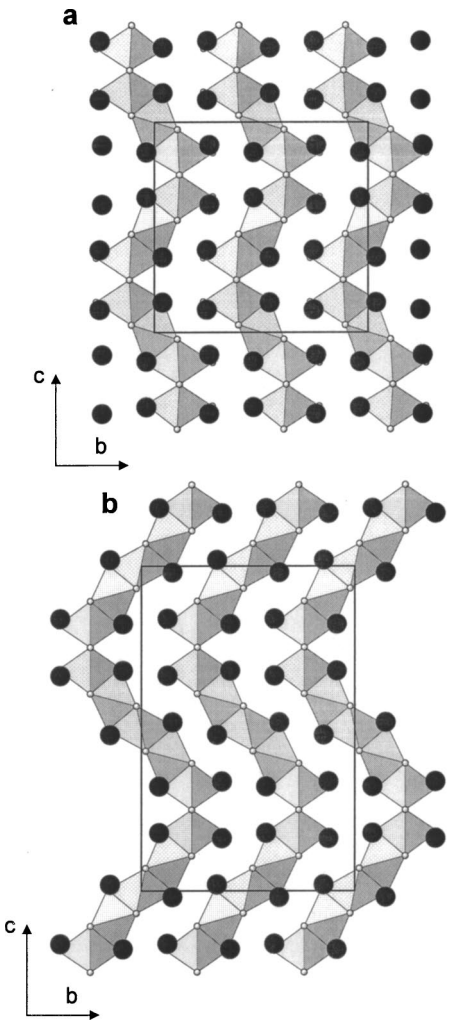

FIG. 1. Schematic representation along the *a* axis of the nuclear structures of (a) $Ba_4Mn_3O_{10}$ and (b) $Ba_6Mn_5O_{16}$. Ba atoms are represented by black dots.

tion is in agreement with the nominal one.

The magnetic susceptibility (dc and ac) was measured in a commercial superconducting quantum interference device magnetometer from Quantum Design (San Diego, USA). The temperature was varied from 1.7 to 800 K; the maximum applied magnetic field was 5 T. The frequency range covered in the ac magnetic susceptibility was from 1 Hz to 1 kHz.

The specific heat was measured by the heat pulse-relaxation method in a commercial cryostat (PPMS, from Quantum Design, San Diego, CA, USA) with a temperature range from 1.7 to 300 K and magnetic fields up to 90 kOe. A pellet of the sample (approximately 15 mg) was attached to a sapphire platform by a small amount of Apiezon N grease. The density of the pellet is close to 90% of the corresponding theoretical value (5.99 g/cc). The addenda heat capacity was measured in a separated run and subtracted from the sample data.

RESULTS

Neutron diffraction data were analyzed by the Rietveld method,[13] using the FULLPROF program.[14] The fitting of the

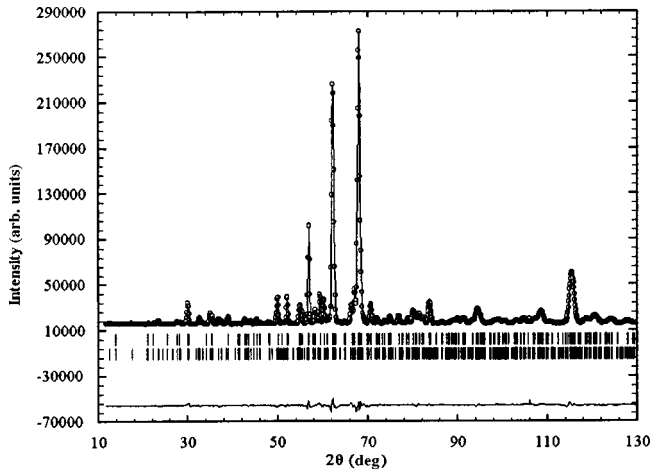

FIG. 2. Graphic result of the fitting of the neutron powder diffraction data of $Ba_6Mn_5O_{16}$ at 2 K: experimental (points), calculated (solid line), and difference (bottom).

experimental patterns at different temperatures up to 110 K was performed using, as starting model for the nuclear structure that one proposed in a previous paper;[11] no additional peaks or scattering contributions to the Bragg peaks of magnetic origin were observed above this temperature. Neutron diffraction patterns recorded below 110 K contain low-angle additional peaks of magnetic origin. These peaks can be indexed in the cell of the nuclear structure, but they are not compatible with the C centering. Figure 2 depicts the graphic result of the fitting of the neutron powder diffraction pattern recorded at 2 K to the nuclear and magnetic structures shown in Figs. 1(b) and 3(a), respectively; the corresponding structural parameters are collected in Table I, whereas Table II shows some selected inter-atomic distances.

The fitting of the neutron diffraction data confirms the model of the nuclear structure previously proposed [Fig. 1(b)]. No vacancies were observed in the cationic sublattice or in the oxygen one. Accordingly, the chemical composition seems to be very close to the nominal one, in agreement with our previous results;[11] therefore, the manganese oxidation state can be assumed to be four. This structure is essentially maintained from room temperature to 2 K, since no structural transition is observed. In this way, Fig. 4 shows the temperature variation of the lattice constants. A continuous decreasing of the parameters is observed down to 80 K, where the variation becomes smaller till lower temperatures. No anisotropic distortion is observed along any crystallographic axis.

The average Mn-O distances are larger than in other Ca (Ref. 15) or Sr (Ref. 16) related manganites, and similar to those found in barium-manganese oxides;[3,9,17] the large size of the barium atoms originates the relax of the Mn-O distances. The (Mn_5O_{18}) units are linked through O(1) which are the common vertices of two $Mn(1)O_6$ octahedra of different (Mn_5O_{18}) units; thus, the only nonshared terminal oxygen is O(2) and, as in $Ba_4Mn_3O_{10}$, this Mn-terminal-oxygen distance is the shortest one in the structure. This short Mn(1)-O(2) distance is compensated for by a large Mn(1)-O(3) one, giving a quite distorted $Mn(1)O_6$ terminal

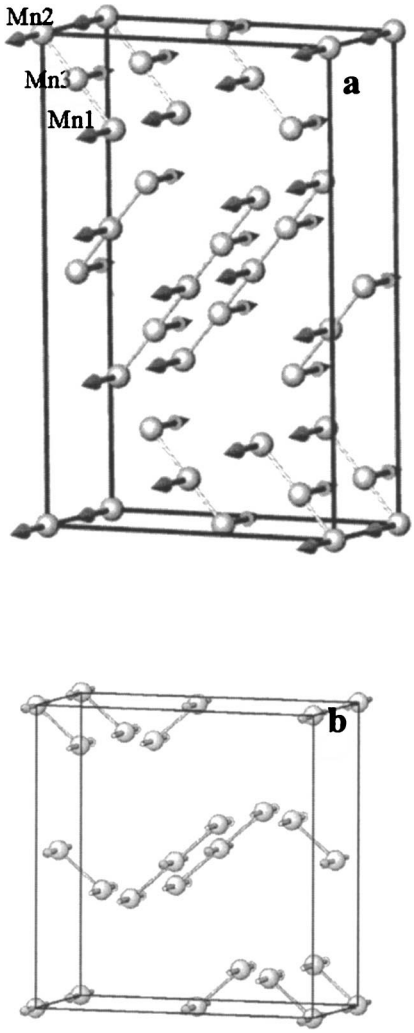

FIG. 3. Magnetic structure of (a) $Ba_6Mn_5O_{16}$ and (b) $Ba_4Mn_3O_{10}$ (see Ref. 9) at 2 K; only Mn cations are shown.

TABLE I. Final structural parameters for the nuclear and magnetic structures of $Ba_6Mn_5O_{16}$ at 2 K. S.G. Cmca(64), a $=0.57230(2)$nm, b$=1.32223(5)$nm, c$=1.99733(8)$nm, V $=1.5114(1)$nm^3, $R_B=0.024$, $R_{exp}=0.007$, $R_{wp}=0.065$, and $\chi^2=16.1$.

Atom	Site	x/a	y/b	z/c
Ba(1)	8f	0	0.1225(7)	0.1625(3)
Ba(2)	8f	0	0.4156(6)	0.1792(4)
Ba(3)	8f	0	0.1452(6)	0.4777(4)
Mn(1)	8f	0	0.2536(7)	0.3122(4)
Mn(2)	4a	0	0	0
Mn(3)	8f	0	0.3816(8)	0.4098(5)
O(1)	8e	1/4	0.2576(6)	1/4
O(2)	8f	0	0.1172(6)	0.3178(4)
O(3)	8f	0	0.4100(6)	0.3142(3)
O(4)	8f	0	0.3563(5)	0.5027(4)
O(5)	16g	0.2268(7)	0.4822(4)	0.4308(2)
O(6)	16g	0.2832(7)	0.2748(4)	0.1139(2)
		Magnetic structure[a]		
atom		position		moment (μ_B)
Mn(1)		(1/2,y,z); (1/2,1/2−y,1/2+z)[b]		−1.98(2)
Mn(1)		(0,y,1/2−z); (0,1/2−y,1/2+z)[b]		1.98(2)
Mn(2)		(0,1/2,1/2)		1.98(2)
Mn(2)		(1/2,1/2,0)		−1.98(2)
Mn(3)		(1/2,y,z); (1/2,−y,−z)[c]		1.98(2)
Mn(3)		(0,y,1/2−z); (0,−y,1/2+z)[c]		−1.98(2)

[a] $a_{mag}=a$, $b_{mag}=b$, $c_{mag}=c$; and $R_{mag}=0.094$; equal and opposite moments at +(1/2,1/2,0).
[b] For Mn(1): y$=0.2536$, z$=0.1878$.
[c] For Mn(3): y$=0.3816$, z$=0.0902$.

octahedra. As shown in Table II, the degree of distortion of the MnO_6 octahedra increases from the center of the (Mn_5O_{18}) unit to its end: the Mn(2) coordination octahedron is almost regular, but that corresponding to Mn(3) is slightly distorted. The regularity is also observed in the metal-metal distances: the two Mn(2)-Mn(3) distances are equal (and short); Mn(3) has a Mn(1) at 2.59 Å besides a Mn(2) at 2.39 Å and, finally, Mn(1) has, as neighboring cations, two Mn(1) at 3.79 Å besides one Mn(2).

The $Ba_6Mn_5O_{16}$ magnetic structure, shown in Fig. 3(a), is quite similar to the corresponding to $Ba_4Mn_3O_{10}$,[9] shown, for comparison, in Fig. 3(b). The spin arrangement depicted in Fig. 3(a) was developed assuming, as in other similar compounds,[9,16] that Mn-Mn interactions are AFM, intrachain interactions being stronger than those between neighboring (Mn_5O_{18}) units. This gives the suppression of the C centering in the magnetic arrangement since the spins related by the translation associated to this centering are antiparallel. In order to keep the number of refined parameters low enough to ensure their reliability, it has been assumed that the ordered magnetic moments of the three crystallographically different Mn cations are equal. This leads to a common value of $1.98(2)\mu_B$, at 2 K. The Mn^{4+} magnetic moment in oxides is very often significantly reduced from the spin-only value ($3.9\mu_B$), mainly due to zero-point and covalence effects.[16] However, the refined value seems to be too low. A low magnetic moment in this compound could be explained on the basis of covalent effects. These effects have also been observed in $Ba_4Mn_3O_{10}$ where trimers (Mn_3O_{12}) exist,[9] to be greater in two-face-sharing MnO_6 octahedra than in the terminal ones. In $Ba_6Mn_5O_{16}$, most (60%) of the MnO_6 octahedra shares two faces; thus, the reduction in the ordered magnetic moments is expected to be important.

The magnetic susceptibility for $Ba_6Mn_5O_{16}$ [see Fig. 5(a) in Ref. 11] obeys a Curie-Weiss law in the temperature range from 500 to 800 K with $\Theta=-774$ K and $\mu_{eff}=4.0\,\mu_B/Mn$. This effective magnetic moment is close to that expected for Mn^{4+} ($3.9\mu_B$), in the spin only approximation. The value of the Weiss constant is very large and negative, indicating strong AFM correlations in the system. In order to shed some light on the magnetic dynamics, ac susceptibility measurements in a range of frequencies from 1 Hz to 1 kHz have also been performed. The observed behavior is rather close to that obtained in the dc susceptibility, i.e., a broad bump centred around 180 K, a clear drop in the susceptibility below 100 K, an increase of the susceptibility

TABLE II. Selected inter-atomic distances (in Å) less than 3.5 Å in $Ba_6Mn_5O_{16}$ at 2 K.

Ba(1)-O(1)	2.880(8)×2	Mn(1)-O(1)	1.895(6)×2
Ba(1)-O(2)^{i}	3.102(9)	Mn(1)-O(2)	1.81(1)
Ba(1)-O(2)^{ii}	2.889(1)×2	Mn(1)-O(3)	2.07(1)
Ba(1)-O(3)	2.85(1)	Mn(1)-O(6)	1.948(8)×2
Ba(1)-O(4)	3.204(1)	Average	1.927(2)
Ba(1)-O(5)	2.932(8)×2	Distortion[a]	$16.8\,10^{-4}$
Ba(1)-O(6)	2.761(8)×2		
Average	2.916(2)	Mn(2)-O(4)	1.901(7)×2
		Mn(2)-O(5)	1.911(2)×4
Ba(2)-O(1)	2.900(9)×2	Average	1.907(2)
Ba(2)-O(2)	2.67(1)	Distortion[a]	$0.06\,10^{-4}$
Ba(2)-O(3)^{i}	2.70(1)		
Ba(2)-O(3)^{ii}	2.866(1)×2	Mn(3)-O(3)	1.95(1)
Ba(2)-O(5)	2.836(8)×2	Mn(3)-O(4)	1.89(1)
Ba(2)-O(6)	2.791(8)×2	Mn(3)-O(5)	1.906(9)×2
Average	2.816(2)	Mn(3)-O(4)	1.938(9)×2
		Average	1.920(4)
Ba(3)-O(2)	3.22(1)	Distortion[a]	$1.30\,10^{-4}$
Ba(3)-O(4)^{i}	2.84(1)		
Ba(3)-O(4)^{ii}	2.888(1)×2	Mn(1)-Mn(1)	3.79(1)×2
Ba(3)-O(5)^{i}	2.937(8)×2	Mn(1)-Mn(3)	2.58(1)
Ba(3)-O(5)^{ii}	2.822(8)×2	Mn(2)-Mn(3)	2.39(1)×2
Ba(3)-O(6)^{i}	2.797(8)×2		
Ba(3)-O(6)^{ii}	3.340(8)×2		
Average	2.968(2)		

[a]Distortion$= 1/n\,\Sigma[d_i - \langle d\rangle)/\langle d\rangle]^2$.

below 20 K and a very weak dependence on frequency.

The specific heat for $Ba_6Mn_5O_{16}$ is shown in Fig. 5(a). A clear peak is observed around 87 K, which would indicate a phase transition. Extra anomalies are observed neither at low temperatures (below 50 K) nor at high temperatures (up to 400 K). In order to connect these anomalies to the magnetic properties, the temperature derivative of the magnetic susceptibility has been calculated and the data included on the same temperature scale in the inset of Fig. 5(a). Since these anomalies clearly coincide, the peak in the specific heat could be due to a transition to a long-range magnetic ordered phase (AFM long range order, $T_N = 87$ K), though a clear peak is not observed in the magnetic susceptibility. These data are in agreement with the temperature dependence of the neutron diffraction data that shows a three-dimensional (3D) AFM ordering for $Ba_6Mn_5O_{16}$. The variation of the ordered magnetic moment with temperature, shown in Fig. 6, suggests for $Ba_6Mn_5O_{16}$ a Neel temperature about 105 K. The displacement in temperature is most likely due to different thermometer calibration.

DISCUSSION

From the magnetic bulk data and the neutron powder diffraction patterns at low temperature, a coherent picture of the magnetic behavior of $Ba_6Mn_5O_{16}$ can be obtained. At temperatures well above 600 K, the system is paramagnetic with the localized moment of the Mn^{4+} ions (spin only approximation). At high temperatures (400–150 K), the system behaves as an AFM spin chain or as some type of dimmer spin pairing, with very strong AFM interactions. This is consistent with the magnetic parameters obtained from the Curie-Weiss behavior in the inverse magnetic susceptibility along this temperature range. At intermediate temperatures (87–150 K), these short range AFM correlations compete with the long range 3D AFM ordering and a complex magnetic cluster behavior is probably created. Moreover, we could propose that zigzag chains couple inside the layer, presenting some type of 2D complex ordering. Finally, below 87 K, a long range 3D AFM ordering is established. Actually, the zigzag chains seem to be strongly coupled in the layer between 87 to 150 K (interchain distance 2.56 Å), as well as between the different layers (below 87 K) giving rise to a 3D AFM structure (interlayer distance 3.8 Å) with $T_N \approx 87$ K. In fact, this Neel temperature coincides with the peak observed in the derivative of the magnetic susceptibility and the peak of the specific heat.

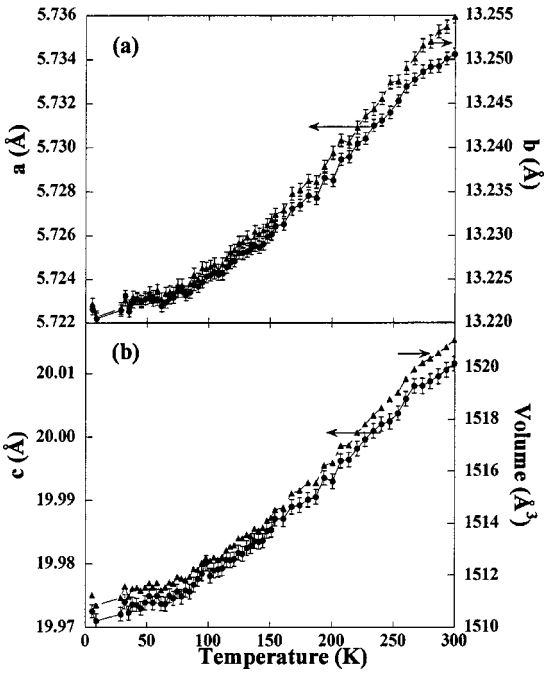

FIG. 4. Variation of (a) *a* and *b* unit cell parameters and (b) *c* axis and cell volume as a function of the temperature.

The magnetic behavior of $Ba_6Mn_5O_{16}$ is related to the 2D nature of the structure, being expected to be similar to that observed in $Ba_4Mn_3O_{10}$.[9] Accordingly, a comparative study can be performed. Actually, the main features are comparable: the low value of the susceptibility, a broad maximum centered around 180 K, the rather sharp drop of the susceptibility below 100 K, and a clear increase in the magnetic susceptibility below 20 K. From the temperature dependence of the inverse of the magnetic susceptibility for $Ba_4Mn_3O_{10}$ (not shown; see Ref. 9), the paramagnetic behavior can be extracted assuming a Curie-Weiss law. The obtained paramagnetic moment is $4.5\mu_B$/Mn and $\Theta = -640$ K. These values are rather unexpected, since the paramagnetic moment is far from the expected value for Mn^{4+} ($3.9\mu_B$/Mn). Besides, the Curie temperature is very high, indicating very strong

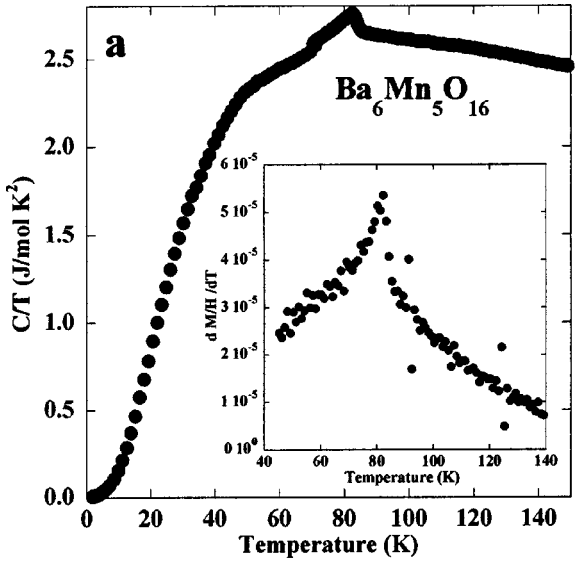

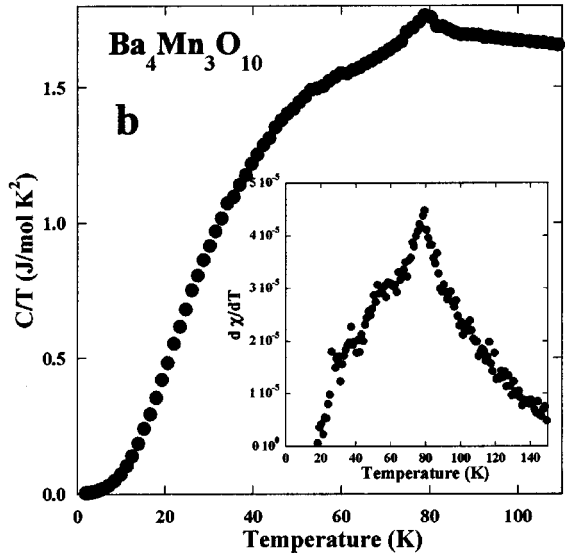

FIG. 5. Temperature dependence of the specific heat for (a) $Ba_6Mn_5O_{16}$ and (b) $Ba_4Mn_3O_{10}$. The inset shows the derivative of the magnetic susceptibility in a similar temperature range.

AFM interactions in the system.

The $Ba_6Mn_5O_{16}$ magnetic structure determined from the neutron diffraction data suggests a strong AFM coupling within the five-octrahedra (Mn_5O_{18}) units, and also an antiferromagnetic coupling between the different layers along [010]. This AFM structure is quite similar to that reported for $Ba_4Mn_3O_{10}$,[9] shown for comparison in Fig. 3(b). In this compound, the intratrimer Mn-Mn interactions are also AFM and stronger that the intertrimer ones that seem to be ferromagnetic. The refinement of the atomic magnetic moments of the two crystallographically different Mn gives $2.23\mu_B$ and $1.96\mu_B$ values. The difference in the ordered magnetic moments of both manganese atoms has been attributed to the different bonding environments experienced by cations in

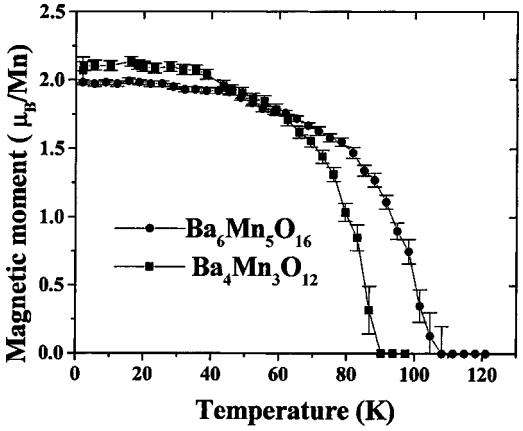

FIG. 6. Temperature dependence of the ordered magnetic moment as obtained from the neutron powder diffraction data for $Ba_6Mn_5O_{16}$ and $Ba_4Mn_3O_{10}$.

octahedra with different linkage patterns; the covalent interactions are greater in an octahedron which shares two faces with the neighboring polyhedra. In $Ba_6Mn_5O_{15}$, the three crystallographically different manganese ions should have also different magnetic moments as a consequence of their different environments. However, due to the limited resolution of our data, we forced the same magnetic moment at the three positions in order to reduce the number of free parameters in the Rietveld fit. The value for the magnetic moment of the manganese atoms is low, 1.98(2) μ_B, probably due to the fact that in $Ba_6Mn_5O_{16}$, the quantity of two-face-sharing octahedra is much higher than in $Ba_4Mn_3O_{10}$.[9]

In order to complete this comparative study we have measured the specific heat for $Ba_4Mn_3O_{10}$ [Fig. 5(b)]. A peak is clearly observed at $T_N = 80$ K. The total specific heat should usually have at least three components: electronic, magnetic, and lattice (phonons). In our case, the first one can be assumed to be negligible. Thus, if the lattice contribution is calculated, it could be subtracted to obtain the magnetic specific heat. The lattice component can be assumed to follow a Debye model (T^3) in the low temperature range. At interme-

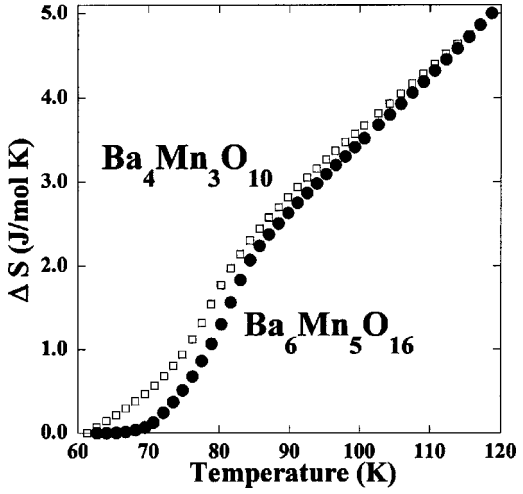

FIG. 7. Temperature dependence of the magnetic entropy at zero magnetic field for $Ba_6Mn_5O_{16}$ and $Ba_4Mn_3O_{10}$.

diate temperatures, the lattice contribution was calculated by considering three Einstein optical modes. The oscillator corresponding to these modes are centred at 100, 450, and 800 K. The specific heat can also be compared in both compounds, around T_N [see Figs. 5(a) and 5(b)]. It is clearly observed that T_N is close in both cases (80 K vs 87 K), the difference in the specific heat being related to the different number of magnetic atoms in each case (also see Fig. 6). To obtain the entropy associated with the AFM ordering the magnetic specific heat was integrated (Fig. 7). The total entropy is much lower than the expected for three or five Mn^{4+} $[s=2(R\ln(2S+1))]$, with $S=3/2$. In particular, the entropy is only 15% ($Ba_4Mn_3O_{10}$) or 9% ($Ba_6Mn_5O_{16}$) of the expected entropy associated with a long range (3D) magnetic phase transition. In principle, this low value could be related to a non-accurate subtraction of the lattice component of the specific heat. Alternatively, this could suggest that some of the spins of the Mn^{4+} ions at the ends of the three or five octahedra units are not strongly correlated to the rest. This fact would show a paramagnetic Curie Weiss tail in the magnetic susceptibility at low temperature, as clearly observed in Fig. 5(a) of Ref. 11.

ACKNOWLEDGMENTS

Financial support through Research Projects Nos. MAT2001-1440 and MAT2002-1329 is acknowledged.

*Email address: jgcalbet@quim.ucm.es. FAX: (34) 91 394 43 52.

[1] R. von Helmot, R. J. Wecker, B. Holzapfel, L. Schultz, and K. Samwer, Phys. Rev. Lett. **71**, 2331 (1993).
[2] Y. Morimoto, A. Asamitsu, H. Kawahara, and Y. Tokura, Nature (London) **380**, 141 (1996).
[3] A. Hardy, Acta Crystallogr. **15**, 179 (1962).
[4] M. Steiner, W. Kruger, and B. Babel, Solid State Commun. **9**, 227 (1971).
[5] T. Negas and R. S. Roth, J. Solid State Chem. **3**, 323 (1971).
[6] J. M. González-Calbet, M. Parras, J. Alonso, and M. Vallet-Regi, J. Solid State Chem. **106**, 99 (1993).
[7] J. M. González-Calbet, M. Parras, J. Alonso, and M. Vallet-Regi, J. Solid State Chem. **111**, 202 (1994).
[8] M. Parras, J. M. González-Calbet, J. Alonso, and M. Vallet-Regi, J. Solid State Chem. **113**, 78 (1994).
[9] V. Zubkov, A. Tyutyunnik, I. F. Berger, V. I. Voronin, G. V. Bazuev, C. A. Moore, and P. D. Battle, J. Solid State Chem. **165**, 454 (2002).
[10] R. Schmidt, J. Pebler, and D. Babel, Eur. J. Solid State Inorg. Chem. **29**, 679 (1992).
[11] K. Boulahya, M. Parras, J. M. González-Calbet, and J. L. Martinez, Chem. Mater. **14**, 4006 (2002).
[12] R. Schmidt and D. Babel, Z. Anorg. Allg. Chem. **516**, 187 (1984).
[13] H. V. Rietveld, J. Appl. Crystallogr. **2**, 65 (1969).
[14] J. Rodriguez-Carvajal, Physica B **192**, 55 (1993).
[15] P. D. Battle, M. A. Green, J. Lago, J. E. Millbrun, M. J. Rosseinsky, and J. F. Vente, Chem. Mater. **10**, 658 (1998).
[16] J. F. Vente, K. V. Kamenev, and D. A. Sokolov, Phys. Rev. B **64**, 214403 (2002).
[17] E. J. Cussen and P. D. Battle, Chem. Mater. **12**, 831 (2000).